ORIGINAL PAPER

RJME Romanian Journal of Morphology & Embryology http://www.rjme.ro/

Beyond H&E: CDX2 immunohistochemistry in tumor budding assessment of colorectal carcinoma

AMINIA DIANA CIOBĂNOIU[1)], GHEORGHE GINDROVEL DUMITRA[2)], IANCU EMIL PLEŞEA[1,3)], ANWAR ERCHID[1)], VALENTIN TITUS GRIGOREAN[1,4)]

[1)]*Doctoral School, Carol Davila University of Medicine and Pharmacy, Bucharest, Romania*
[2)]*Department of Family Medicine, University of Medicine and Pharmacy of Craiova, Romania*
[3)]*Department of Pathology, Bagdasar–Arseni Emergency Clinical Hospital, Bucharest, Romania*
[4)]*Department of Surgery, Carol Davila University of Medicine and Pharmacy, Bucharest, Romania*

Abstract

Background and Objectives: Tumor budding (TB) phenomenon is recognized as one of the important adverse prognostic factors of colorectal carcinoma (CRC) and is currently assessed following to the *International Tumor Budding Consensus Conference* (ITBCC) recommendations on routine Hematoxylin and Eosin (H&E)-stained slides. However, TB evaluation may become difficult in cases showing inflammatory infiltrates, stromal desmoplasia, or glandular fragmentation. Immunohistochemical (IHC) markers, including caudal type homeobox 2 (CDX2), may improve the identification of isolated tumor buds in such situations. *Patients, Materials and Methods*: The retrospective study included 170 CRC cases selected from the archives of a single regional pathology center. TB was evaluated on both H&E-stained and CDX2-immunostained slides according to a modified *ITBCC*-based grading system including an additional Bd0 category for cases lacking identifiable tumor buds. Tumor buds were counted within a standardized field area. TB distribution was evaluated in the proximal, middle, and distal tumor regions. *Results*: Low-grade budding lesions predominated in all evaluated tumor regions on both H&E and CDX2 assessment. Regional variation in TB distribution was observed along the invasive tumor front, supporting the presence of spatial heterogeneity in CRC. Comparative analysis of TB evaluation on H&E-stained preparations and on CDX2 immunolabeled preparations revealed the existence of differences between the two methods, especially in cases with low or intermediate budding activity. CDX2 immunostaining facilitated the identification of additional tumor buds, leading to the reclassification of a number of cases to higher budding categories (intermediary and high-grade budding lesions), especially in difficult cases, characterized by intense stromal reaction, inflammation or glandular fragmentation. *Conclusions*: The present study demonstrated that IHC labeling should be considered primarily as a detection tool for accurate TB assessment, but other antibodies should be tested to increase the accuracy of tumor bud identification.

Keywords: larynx, colon adenocarcinoma, tumor architecture, histopathology, mucinous adenocarcinoma, tumor grading.

Introduction

Colorectal carcinoma (CRC) is still one of the leading causes of morbidity and mortality in cancer all over the world [1]. In addition to conventional clinicopathological parameters [tumor stage, lymph node (LN) involvement, and histological grade], tumor budding (TB) has gained increasing attention due to its association with aggressive tumor behavior and unfavorable clinical outcome.

TB's prognostic significance is particularly important in pT1 CRC, where it plays a major role in therapeutic decision-making. In early CRCs treated by local excision, TB of high-grade has been strongly related with an increased risk of local recurrence LN involvement, frequently representing an indication for additional surgical treatment. A meta-analysis including more than 24 000 pT1 CRC cases confirmed that high-grade TB is a strong predictor of both local recurrence and LN metastases in pT1 lesions [2].

TB also demonstrates important prognostic implications in stage II CRC. Several studies prove that high-grade TB is related to increased risk of tumor recurrence, reduced disease-free survival interval, and unfavorable overall survival (OS) in stage II tumors. Due to its prognostic value, high-grade TB is currently considered an additional adverse risk factor that may contribute to adjuvant treatment decision-making in stage II CRC patients [3, 4].

Owing to its growing clinical relevance, *International Tumor Budding Consensus Conference* (ITBCC) established a set of standardized recommendations for TB evaluation and reporting in CRC [5]. Prior to the publication of the *ITBCC* guidelines, marked variability existed among studies regarding the definition of tumor buds, counting methodology, magnification fields, and grading systems, resulting in reduced reproducibility and limited implementation in routine pathology practice.

According to the *ITBCC* criteria, TB is defined as the presence of isolated single tumor cells or clusters composed of up to four tumor cells located at the invasive front of the tumor [5].

Assessment is performed on slides stained with Hematoxylin and Eosin (H&E) by initially identifying the hotspot area with the highest budding density at low magnification, followed by counting of tumor buds inside a standard field area of 0.785 mm^2 at ×20 objective magnification.

This is an open-access article distributed under the terms of a Creative Commons Attribution-NonCommercial-ShareAlike 4.0 International Public License, which permits unrestricted use, adaptation, distribution and reproduction in any medium, non-commercially, provided the new creations are licensed under identical terms as the original work and the original work is properly cited.

Based on the number of identified tumor buds, cases are classified into three categories: low-grade TB – Bd1 (0–4 buds), intermediate-grade TB – Bd2 (5–9 buds), and high-grade TB – Bd3 (≥10 buds).

Some studies proposed the introduction of an additional Bd0 category for CRCs showing complete absence of TB [6, 7]. While the current *ITBCC* recommendations classify low-grade budding as Bd1 (0–4 buds), this modified approach separates tumors with no detectable buds from those showing low but present budding activity. The rationale behind this proposal was based on the observation that the Bd1 category includes a heterogeneous group of tumors, ranging from cases with complete absence of budding to lesions exhibiting up to four tumor buds. By distinguishing these categories, the authors suggested that a more refined subclassification of low-budding CRCs could be achieved.

Even though the *ITBCC* recommendations standardized TB assessment on routine H&E-stained slides, several limitations may still be encountered during evaluation, particularly in cases showing prominent inflammatory infiltrates, stromal desmoplasia, glandular fragmentation, or poorly preserved morphology. In such situations, the identification of isolated tumor buds may become difficult, leading to potential interobserver variability and discrepancies in TB quantification. The use of immunohistochemistry remains mainly adjunctive, particularly in morphologically difficult cases. Some studies demonstrated that immunohistochemical (IHC) evaluation may facilitate hotspot identification and improve visualization of isolated tumor buds [8]. Pan-cytokeratin (CK) IHC stains are most commonly used in TB assessments, particularly in cases showing intense inflammatory infiltrates, stromal desmoplasia, glandular fragmentation, mucin pools, or poorly preserved morphology, where the identification of isolated tumor buds on H&E sections may become challenging.

Growing interest has been directed toward the relationship between TB biology and caudal type homeobox 2 (CDX2) expression in CRC. Unlike pan-CK IHC stains, which highlight the entire cytoplasm of tumor cells, CDX2 demonstrates a distinct nuclear staining pattern, potentially facilitating the differentiation of true tumor buds from surrounding stromal or inflammatory cells. Several authors observed that smaller tumor clusters and tumor buds may show progressive reduction or heterogeneous CDX2 expression, particularly at the invasive front of CRCs. These findings suggest that alterations in CDX2 expression may reflect the dynamic morphological and molecular changes occurring during tumor progression and TB formation [9].

However, IHC assessment may increase the total number of identified buds and potentially lead to overestimation, particularly in areas showing glandular fragmentation or pseudo-budding phenomena. Unlike true TB, pseudo-budding represents isolated tumor cells or small cell clusters resulting from gland rupture and inflammatory-related tissue disruption rather than genuine invasive budding activity [10–12].

In contrast, reduced or absent CDX2 expression has been correlated with aggressive tumor behavior, poorly differentiated status, advanced tumor stage, LN involvement, microsatellite instability (MSI), and unfavorable clinical outcome. Several molecular studies suggested that loss of CDX2 expression may reflect progressive dedifferentiation and molecular alterations involved in colorectal carcinogenesis [10, 11].

Aim

The authors aimed in this study to compare TB assessment on conventional H&E-stained slides and CDX2-immunostained sections in CRC and to evaluate the concordance between the two assessment methods.

Patients, Materials and Methods

Study design and participants

This study group included 170 cases diagnosed with and operated on for CRC in a single medical institution for three years.

Excluding criteria

Patients who received neoadjuvant chemoradiotherapy, as well as cases involving adenomatous lesions, mesenchymal, lymphoid, or neuroendocrine tumors, were excluded from the study.

The study was carried out in a single medical center, with a prospective component regarding the sampling of the studied material and a retrospective component regarding data collection from patients' medical documents and data provided by histologically processed tissue fragments.

The retrieval of archived tissue material and clinical data was performed in accordance with the ethical regulations and approvals applicable to the present study.

Studied parameters

There were two categories of parameters:

- Clinical data, including age and sex.
- Morphological data, including tumor location, histological type, differentiation grade, local invasion (pT stage) and budding status.

Histopathological evaluation

All surgical specimens were grossed according to a standardized sampling protocol. One longitudinal section was obtained from the proximal tumor area, one from the central/middle portion of the lesion, and one from the distal tumor front (Figure 1), while the remaining tumor tissue was serially sampled through transverse sections in order to ensure adequate evaluation of tumor architecture, depth of invasion, and invasive front morphology.

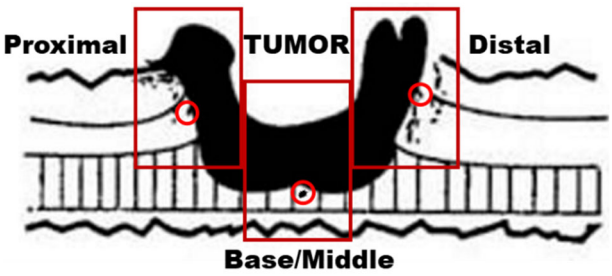

Figure 1 – ***Schematic representation of the gross sampling protocol used for tumor budding assessment.***

Representative tissue sections were subsequently subjected to classical histological processing techniques (fixation in 10% neutral buffered formalin, and paraffin embedding)

and stained further with H&E in order to obtain guide slides (Figure 1).

H&E-stained slides were reviewed in all cases in order to assess the histological subtype, histological grade according to the four-tier grading system recommended by *College of American Pathologists* (CAP) protocols [12], tumor extent, and TB status.

Next step was the identification and marking of TB areas at the invasion front on the guide slides and, then on the paraffin blocks (Figure 2). When marking the areas, it was considered that the marked area also contained a fragment of tumor tissue at the invasion front.

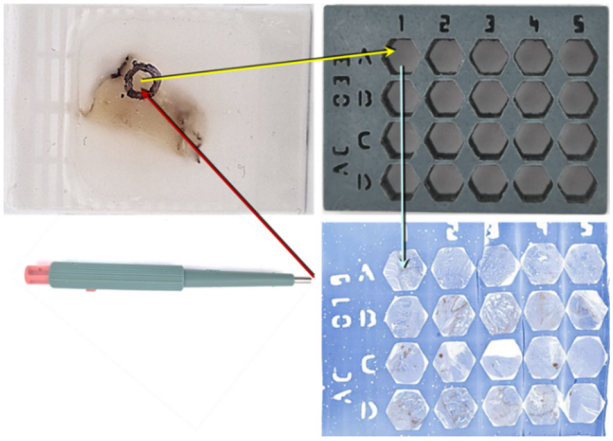

Figure 2 – ***TMA construction protocol used for CDX2 IHC assessment. CDX2: Caudal type homeobox 2; IHC: Immunohistochemical; TMA: Tissue microarray.***

The next step was the building, following a special protocol [13, 14], of tissue microarray (TMA) blocks from TB hotspot areas identified in the proximal, middle, and distal tumor regions on H&E slides and extracted from the primary blocks with a special puncher of 3 mm diameter (Figure 2).

From TMA blocks was cut a 2 mm paraffin section that was stretched on a special Superfrost™ Plus slide and immunomarked with CDX2 (monoclonal mouse anti-human antibody, clone DAK–CDX2, from Agilent Technologies), after heat induced epitope retrieval in Ethylenediaminetetraacetic acid (EDTA) buffer.

Both H&E and CDX2 slides were digitized with a P480 scanner from 3DHISTECH, using the ×40 lens.

TB assessment was performed according to the *ITBCC* recommendations [5], but with a modified grading approach incorporating an additional Bd0 category for tumors lacking identifiable tumor buds (Table 1).

Table 1 – ***Budding score scale***

Budding score	Description	Grading
No budding	0 Tumor buds	Bd0
Low	1–4 Tumor buds	Bd1
Intermediary	5–9 Tumor buds	Bd2
Increased	>10 Tumor buds	Bd3

The invasive tumor front was initially scanned at low magnification in order to identify the hotspot areas with the highest budding density.

Tumor buds, defined previously, were counted on both H&E and CDX2 digital slides inside a standard field area of 0.785 mm^2 at ×20 objective magnification, using Slide Viewer 2.9 software from 3DHISTECH.

Statistical analysis

The comparison of TB scores between the two stains in the proximal (T_P), middle (T_M), and distal (T_D) tumor regions was realized with the χ^2 (*chi*-squared) test.

Graphical representations of the data were created using the "Graph" tools available in the "Excel" module of Microsoft Office 2019 Professional, and the XLSTAT 2014 add-in software for Microsoft Excel (trial version).

Results

Clinicopathological profile

The studied group consisted of 170 patients diagnosed with CRC, with an average age of around 66 years.

All clinicopathological characteristics of the patients included in the study are presented in Table 2.

Table 2 – ***Clinicopathological characteristics of the cohort***

Variable		*n* (%)
No. of cases		170
Mean age [years]		66.46±10.77
Sex	Male	99 (58.23%)
	Female	71 (41.77%)
Tumor location	Right colon	58 (34.12%)
	Transverse colon	21 (12.35%)
	Left colon	62 (36.48%)
	Rectum	29 (17.06%)
Histological subtypes		
Adenocarcinoma	Conventional	142 (83.53%)
	Adenoma-like	5 (2.94%)
	Mucinous	4 (2.35%)
	With mucinous component	17 (10%)
Other types	Micropapillary	1 (0.59%)
	Medullary carcinoma	1 (0.59%)
Histological grade	G1	71 (42%)
	G2	75 (44%)
	G3	24 (14%)
pT stage	pT2	77 (45%)
	pT3	93 (55%)

More than half of these patients were older than 65 years and there was no patient younger than 29 years. Male patients predominated, with almost two-thirds of the patients. The most frequently involved tumor locations were the left and right colon, while rectal and transverse colon tumors gathered together less than on third of the cases.

Conventional adenocarcinoma (ADK) represented the predominant histological subtype, and together with the five cases of adenoma-like form, accounted for almost 90% of the cases. Mucinous ADK was rare but mixed histological type of ADK and mucinous carcinoma were identified quite frequently. Other particular types, as micropapillary ADK and medullary carcinoma were identified only in a limited number of cases.

Most tumors were classified as moderately or well differentiated, while poorly differentiated carcinomas accounted for less than 15% of the cases. Although medullary carcinoma is no more conventionally graded according to the last standard glandular differentiation criteria [1], we considered it as a poorly differentiated tumor and included in the corresponding group of our series. Tumors extended

beyond the colonic wall (pT3) were slightly more frequent than tumors confined to the muscular layer (pT2).

Budding assessment

Following the evaluation of clinicopathological characteristics, TB assessment was performed on both H&E and CDX2 IHC slides.

H&E stain

On H&E-stained slides (Figure 3, a–c), Bd1 budding type represented the predominant budding category in all three tumor regions. The middle tumor region, at the base of the tumor, demonstrated the highest number of Bd2 lesions and the lowest number of Bd0 (without budding) cases, suggesting relatively increased budding activity compared with the proximal and distal tumor regions. High-grade budding (Bd3) remained infrequent and showed only minimal variation between the main topographic regions of the tumors (Figure 4a).

The weighted distribution of TB grades demonstrated predominance of the Bd1 category in all three tumor regions, while Bd2 and Bd3 categories accounted for a smaller proportion of cases (Figure 4b).

It is also interesting to point out that TB is lacking in between 20% of cases in the base region of the tumor and 30% in its distal region (Figure 4b).

Overall, however, the differences between the distribution of budding scores in the three main regions of the tumor (proximal, base and distal) were not significant, a fact also confirmed by the statistical apparatus (the *p*-value of the χ^2 correlation test being 0.397, higher than the reference value of 0.05.

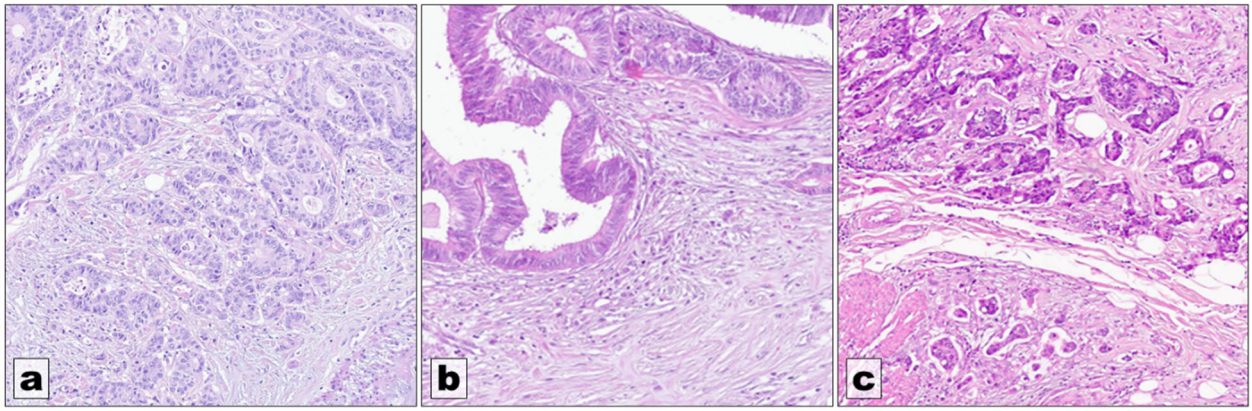

Figure 3 – ***Tumor budding on H&E stain: (a) Score 1; (b) Score 2; (c) Score 3. H&E: Hematoxylin and Eosin.***

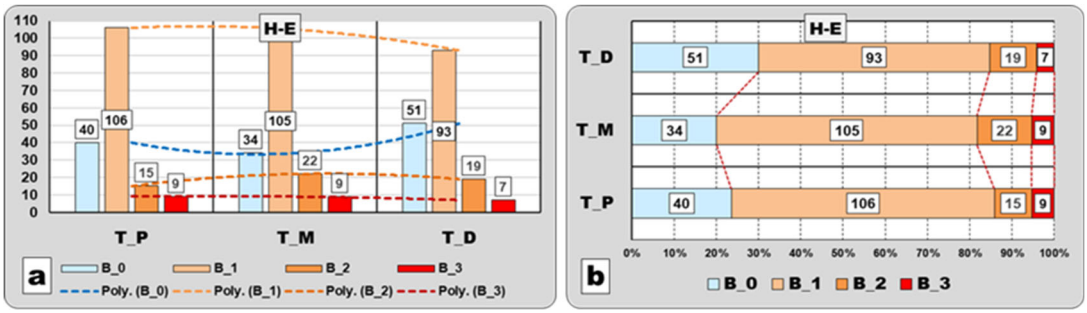

Figure 4 – ***Budding classes assessed on H&E-stained samples in the three tumoral main regions: (a) Distribution; (b) The weight.***

CDX2 IHC stain

First observation obvious on CDX2-immunostained slides was that both the number and the percentage of cases without budding increased in all three regions of the tumors (up to between 30% and 35%). The values increased also discreetly and continuously from the proximal to the distal regions of the tumor.

Then, the second observation was that Bd1 remained the predominant budding category in all tumor regions, but in a lesser extent than in H&E stains because of a slightly increased number of Bd2 and Bd3 cases, particularly within the proximal (the former) and middle (the latter) tumor regions. The distal tumor sector demonstrated the highest number of Bd2 lesions, while the proximal region showed the highest number of Bd3 cases (Figure 5, a–c; Figure 6a).

Overall, however, and in the case of budding score determinations on CDX2 immunolabeled preparations, the differences between the distribution of budding score frequencies in the three main sectors of the tumor (proximal, base and distal) were not significant, a fact also confirmed by the statistical apparatus (the *p*-value of the χ^2 correlation test being 0.834, much higher than the reference value of 0.05, which indicates almost similar distributions of the different budding scores at the level of the three main topographical regions of the tumor (Figure 6, a and b).

Comparison between the two stains results

Proximal region

Comparative evaluation of TB grades in the proximal tumor region demonstrated differences between conventional H&E assessment and CDX2 IHC evaluation. Bd1 represented the predominant budding category using both assessment methods. However, CDX2 immunohisto-chemistry demonstrated a relative decrease in Bd1 lesions

associated with increased numbers of Bd2 and Bd3 cases compared with conventional H&E evaluation (Figure 7a).

Also noteworthy is the higher number of cases in which IHC staining did not reveal the budding process.

The weighted distribution of TB grades further illustrates this shift toward higher budding categories on CDX2-immunostained slides. In particular, CDX2 assessment demonstrated increased relative representation of intermediate- and high-grade budding lesions, suggesting improved visualization of isolated tumor buds in comparison with routine H&E assessment. These findings may reflect the ability of CDX2 immunohistochemistry to facilitate the identification of small tumor clusters and isolated tumor cells within the invasive front.

The weighted distribution of TB grades revealed, secondly, in addition to the increase in Bd2 and Bd3 categories (intermediate and high-grade) in the CDX2 assessment, a corresponding relative decrease in the proportion of non-budding areas and low-grade budding lesions.

These differences in highlighting the TB phenomenon by the two stains were also confirmed statistically, the *p*-value of the χ^2 correlation test being <0.0001, much lower than the reference value of 0.05.

Overall, these observations would suggest that IHC labeling allows for improved and accurate visualization of the TB phenomenon from the proximal region of the tumor (Figure 7b).

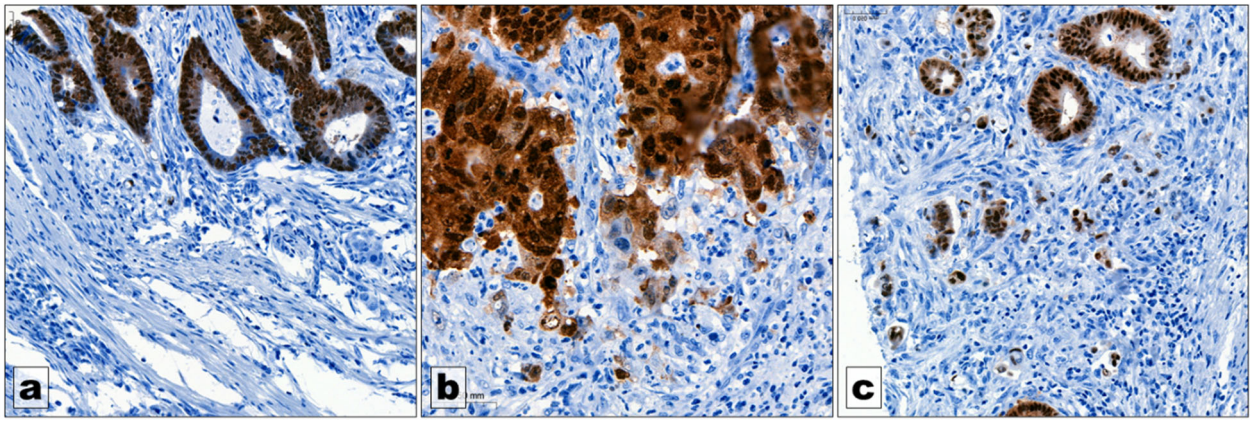

Figure 5 – ***Tumor budding on CDX2 immunostaining: (a) Score 1; (b) Score 2; (c) Score 3.***

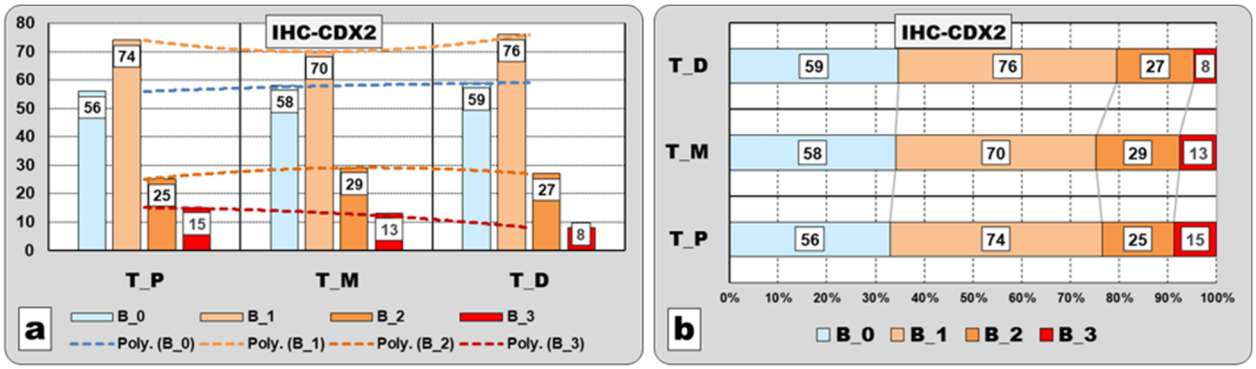

Figure 6 – ***Budding score classes assessed on CDX2 immunomarked samples in the three tumoral main regions: (a) Distribution; (b) The weight.***

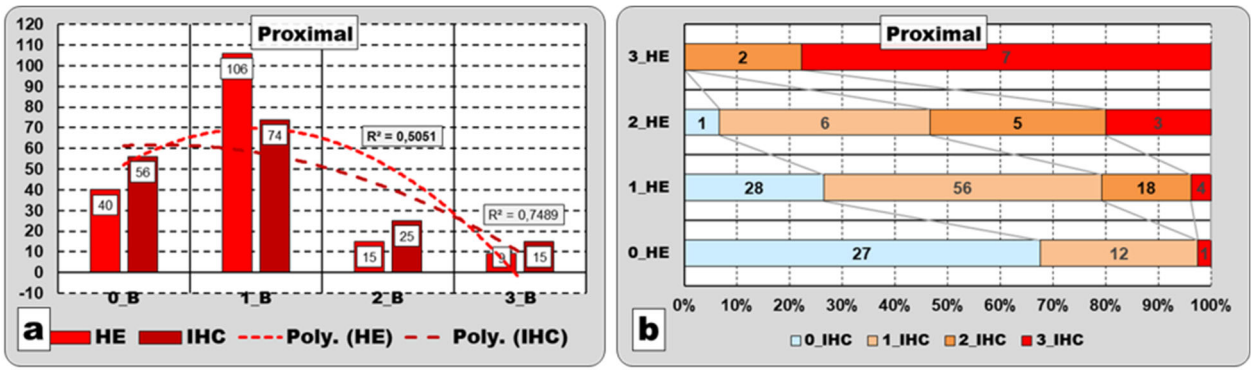

Figure 7 – ***Comparison between budding score classes assessed on the two types of stains in proximal region of the tumors: (a) Distribution; (b) Degree of superposition.***

The degree of agreement between the H&E and CDX2 IHC evaluations demonstrated variable differences between the TB phenomenon scores identified by the two types of marking.

Thus, H&E staining, although it recorded the highest percentage of agreement with the IHC marking regarding the absence of the TB phenomenon, showed, on the other hand, a significant percentage, of almost a third of the determinations in which it underestimated the appearance of tumor buds that were detected by the IHC marking. It is true that the IHC score was low Bd1 (Table 3).

Table 3 – ***Degree of agreement between the two staining procedures in the proximal region***

Budding score concordance formula	Calculus	Concordance degree [%]	Overrated [%]	Underscored [%]
0_B_IHC×100/0_B_H&E	27×100/40	67.5	0	**32.5**
1_B_IHC×100/1_B_H&E	56×100/106	52.8	26.4	20.8
2_B_IHC×100/2_B_H&E	5×100/15	33.3	46.7	20
3_B_IHC×100/3_B_H&E	7×100/9	**77.8**	22.2	0

H&E: Hematoxylin and Eosin; IHC: Immunohistochemical.

For the Bd2 and Bd3 scores evaluated on H&E, the degree of agreement decreased significantly compared to the IHC evaluation, reducing even to half compared to Gd0, increasing instead the degree of overestimation and reducing the degree of underestimation which still remains at a percentage of 20%.

Finally, the highest degree of concordance was recorded at the highest score, Bd3, where, although the number of cases recorded in H&E staining was small (nine cases), two of them were overestimated.

Basal region

Comparative analysis between conventional H&E and CDX2 IHC assessment of TB grades showed that there were also significant differences in the mid-tumor region (at the base of the tumor). Bd1 remained the predominant budding category identified using both assessment methods.

However, CDX2 immunoassayed slides showed, as at the proximal pole, a lower number of Bd1 lesions but an increased number of cases with the lack of TB phenomenon at the tumor invasion front and a higher number of cases with Bd2 and Bd3 scores compared to the H&E assessment (Figure 8a).

The weighted distribution of TB grades was almost similar to that observed at the proximal pole of the tumor (Figure 8b) highlighting here also an increase in the identification of intermediate and high-grade budding lesions which, as previously mentioned, suggests an improved visualization of isolated tumor buds compared to routine evaluation on H&E-stained slides.

The differences in highlighting the budding phenomenon by the two stains were statistically confirmed also at the base of the tumor, the *p*-value of the χ^2 correlation test being <0.0001, much lower than the reference value of 0.05.

The weighted distribution of TB grades highlighted, secondly, here also, in the CDX2 evaluation, a corresponding relative decrease in the share of areas without budding and of low-grade budding lesions. This observation also supports the claim that IHC labeling allows for improved and more accurate visualization of the budding phenomenon also from the tumor region at the base of the tumor.

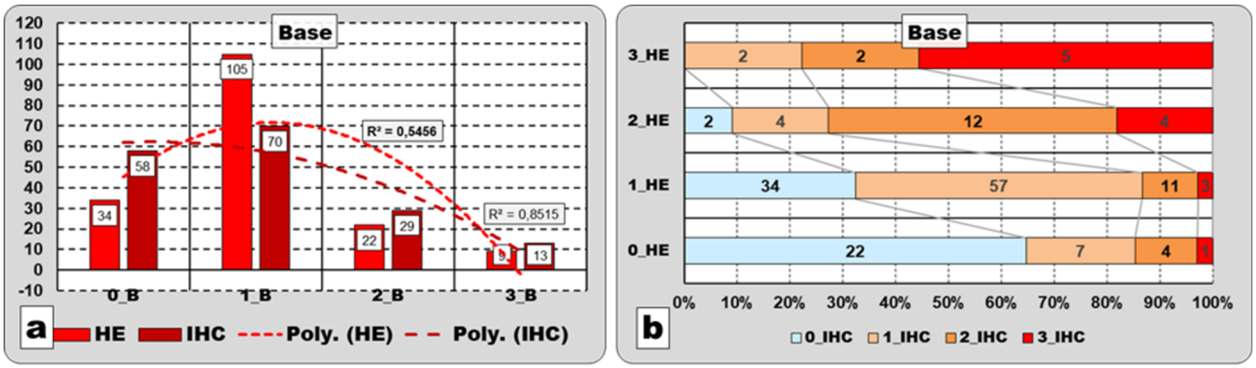

Figure 8 – ***Comparison between budding score classes assessed on the two types of stains in basal region of the tumors: (a) Distribution; (b) Degree of superposition.***

In base of the tumor region also, the **degree of agreement** concordance between the H&E and CDX2 IHC evaluation demonstrated variable differences between the budding scores highlighted by the two types of labeling.

Thus, the H&E staining, although it recorded the highest percentage of concordance with the IHC labeling regarding the absence of budding, showed, on the other hand, a significant percentage, over a third of the determinations, in which it underestimated the appearance of tumor buds that were detected by the IHC labeling. It is worth noting that the IHC score was even Bd3 in one case (Table 4; Figure 8b).

For Bd1–Bd3 scores evaluated on H&E, the degree of concordance compared to the IHC evaluation clearly decreased compared to Gd0 by around 16%, but on the other hand the degree of overestimation increased to around 45% for the Bd3 score and the degree of underestimation decreased but only to a percentage of 18% (Table 4).

Distal region

Finally, comparative assessment of TB grades in the distal tumor region demonstrated differences between conventional H&E and CDX2 IHC assessment.

Bd1 remained the predominant budding category using both methods, although CDX2 immunoassayed slides revealed a lower number of Bd1 lesions associated with an increased representation of Bd0, Bd2, and Bd3 categories compared with H&E assessment.

The weighted distribution of TB grades further illustrates this shift toward higher budding categories in the CDX2 assessment. In particular, intermediate-grade budding lesions (Bd2) were identified more frequently in the IHC assessment, suggesting improved visualization of isolated tumor buds and small tumor clusters in the distal tumor region. High-grade budding lesions (Bd3) remained relatively rare, although slight variations were observed between the two methods (Figure 9, a and b).

Table 4 – ***Degree of agreement between the two staining procedures in the base region***

Budding score concordance formula	Calculus	Concordance degree [%]	Overrated [%]	Underscored [%]
0_B_IHC×100/0_B_H&E	22×100/34	**64.7**	0	**35.3**
1_B_IHC×100/1_B_H&E	57×100/105	54.3	32.4	13.33
2_B_IHC×100/2_B_H&E	12×100/22	54.5	27.3	18.2
3_B_IHC×100/3_B_H&E	5×100/9	55.6	**44.4**	0

H&E: Hematoxylin and Eosin; IHC: Immunohistochemical.

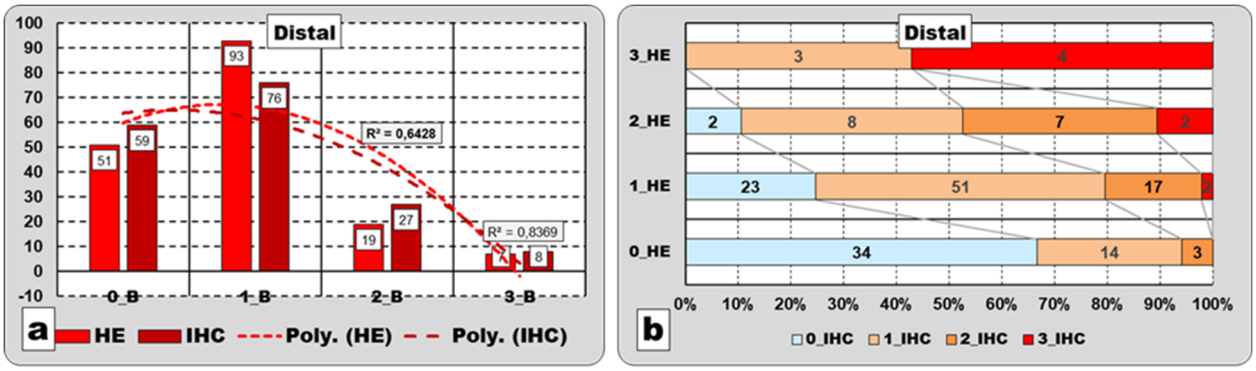

Figure 9 – ***Comparison between budding score classes assessed on the two types of stains in distal region of the tumors: (a) Distribution; (b) Degree of superposition.***

The differences in highlighting the TB phenomenon by the two stains were also statistically confirmed at the distal pole of the tumor, the *p*-value of the χ^2 correlation test being <0.0001, much lower than the reference value of 0.05.

Overall, the observed results support the presence of regional heterogeneity in the distribution of TB and suggest that CDX2 immunohistochemistry may facilitate the identification of additional tumor buds compared to routine H&E evaluation, especially in borderline or intermediate lesions.

The degree of agreement between H&E and CDX2 IHC assessment in the distal tumor region demonstrated variable overlap between the TB categories assessed (Table 5).

Table 5 – ***Degree of agreement between the two staining procedures in the distal region***

Budding score concordance formula	Calculus	Concordance degree [%]	Overrated [%]	Underscored [%]
0_B_IHC×100/0_B_H&E	34×100/51	66.7	0	**33.3**
1_B_IHC×100/1_B_H&E	51×100/93	54.8	24.8	20.4
2_B_IHC×100/2_B_H&E	7×100/19	36.8	52.6	10.6
3_B_IHC×100/3_B_H&E	4×100/7	57.1	**42.9**	0

H&E: Hematoxylin and Eosin; IHC: Immunohistochemical.

The highest agreement was observed for the Bd0 category, followed by Bd3 lesions, while Bd2 demonstrated the lowest agreement rate among the budding groups assessed. Bd1 lesions showed moderate agreement between the two assessment methods.

In contrast, lesions demonstrating complete absence of TB or high-grade budding activity showed comparatively better concordance between H&E and CDX2 assessment.

Overall, the results demonstrate a moderate degree of overlap between the two assessment methods in the distal tumor region.

Discussions

TB, as adverse prognostic factor, is currently considered one of the most important in CRC and has been related with local recurrence, LN involvement, and reduced OS [15].

The *ITBCC* recommendations [5] have standardized the evaluation of TB on H&E-stained slides, improving reproducibility and facilitating its implementation in routine pathology practice.

However, the assessment of TB on H&E-stained slides can become difficult in cases where the malignant proliferation is accompanied by intense peritumoral inflammation or shows stromal reaction or has poorly preserved morphology or glandular fragmentation.

These observations led to the idea of using IHC markers for tumor cells, such as pan-CKs, to increase the accuracy of identifying the budding phenomenon by facilitating the identification of isolated tumor cells and small tumor clusters.

Starting from these premises, the goal of our study was simultaneous labeling, on serial sections, of tumor fragments with H&E and with a tumor marker specific to malignant cells of colon tumors. The marker we have chosen was

CDX2 because it is the most commonly used for the identification of ADKs originating in the gastrointestinal tract and especially those with colorectal localization and presents the advantage of a distinct nuclear staining pattern that could facilitate the identification of isolated tumor buds and their distinction from surrounding stromal or inflammatory cells [16].

Comparison of the obtained results showed a reduced identification of low TB scores by IHC labeling due, on the one hand, to the increase in the percentage of cases in which classical staining erroneously identified isolated cells or small groups of cells belonging to the immune or stromal cell compartment in this area as malignant cells, probably due to increased cell densities of the cell populations in the mentioned compartments at the level of the invasion front (Figure 10).

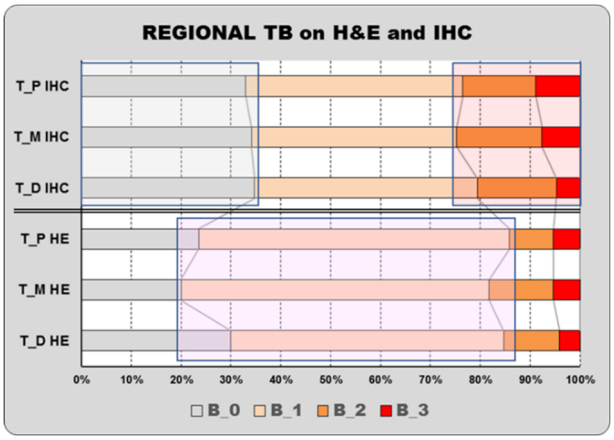

Figure 10 – ***The differences between the two staining methods.***

On the other hand, it better highlighted some tumor buds, especially those formed by isolated cells or small groups of cells, contributing to an increase in the percentages of high budding scores (Figure 10 – right).

The adjustment of the identification of the budding phenomenon and the distribution of its intensity degrees was found at the level of all three topographical regions of the tumor.

Thus, at the level of the **proximal region of the tumor**, the analysis of the degree of match between the recordings of the TB phenomenon using the two staining techniques revealed that almost a third of the cases evaluated as lacking budding on H&E (13 out of 40 cases) were underestimated, CDX2 labeling identifying tumor buds, it is true with a low score.

IHC labeling refuted a little over a quarter of the cases considered to present a low-grade budding phenomenon on H&E staining and overestimated the score of a little over 20% of the same cases evaluated as low-grade on H&E staining. Also, one case evaluated as Bd2 on H&E was negative by IHC.

The largest discrepancies were recorded in cases identified with a Bd2 score on H&E, with the lowest percentage of concordance and the highest percentage of overestimation compared to IHC staining (Table 3).

At the **tumor base** level, analysis of the degree of overlap between the recordings of the TB phenomenon using the two staining techniques revealed that more than a third of the cases evaluated as lacking budding on H&E (12 out of 34 cases) were underestimated, with CDX2 staining identifying tumor buds, some with scores higher than Bd1.

IHC staining refuted almost a third of the cases considered to present a low-grade budding phenomenon on H&E staining and overestimated the score of almost 15% of the same cases evaluated as low-grade on H&E staining. Also, one case evaluated as Bd2 on H&E was negative on IHC.

The largest discrepancies were recorded in cases identified with a Bd2 score on H&E, with the lowest percentage of concordance and the highest percentage of overestimation compared to IHC staining.

Among the cases classified as Bd2 in the H&E evaluation, almost half (45.5%) were redistributed on the CDX2 immunoassayed slides to different budding scores, either lower or higher.

Finally, almost half of the cases classified as Bd3 on the H&E-stained slides were overestimated, being downgraded to lower scores by the IHC staining (Table 4).

At the **distal pole of the tumor**, analysis of the degree of overlap between the TB recordings using the two staining techniques revealed that approximately one third of the cases evaluated as without TB on H&E (17 out of 51 cases) showed TB on the CDX2 immunoassayed slides.

Almost half of the lesions classified as Bd1 in the H&E evaluation (45.2%) were reassigned to different budding categories after the CDX2 evaluation, almost one third of the cases quarter being downgraded as a score to Bd0, and just over 20% being overestimated as a score, especially Bd2 but also Bd3.

Bd2 lesions demonstrated the smallest range of overlaps between the two methods, namely just over a third of the cases. The remaining almost two-thirds of the cases being reclassified following IHC evaluation, most often downgraded as a score by one class (respectively to Bd1).

It is also worth noting that a significant subset of cases identified in the H&E evaluation as having a Bd3 score showed lower budding grades on CDX2 immunoassayed slides, which supports the presence of a significant discordance between the conventional and IHC assessment of TB and the cause of high-grade budding scores (Table 5).

Finally, it can be stated that, as illustrated in Figure 11, in about a quarter of the cases stained with H&E, the TB phenomenon was not identified in all three topographic regions of the tumors.

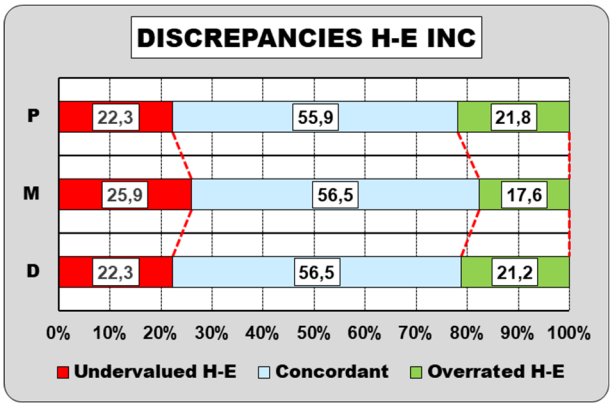

Figure 11 – ***The degree of overlap between the two staining methods.***

The degree of actual concordance between the two stains was between 55% and 57%, which, together with the

situations described previously, constitutes a solid argument in favor of using IHC labeling as a routine method for identifying and quantifying the TB phenomenon. Even the relatively significant percentage of cases overestimated on the H&E staining signals the ability to adjust the evaluation of the intensity of the budding phenomenon by using IHC labeling.

Although our study showed an improvement in the identification and classification of TB using IHC markers specific for colon cancer cells compared to the identification and evaluation of the phenomenon on H&E-stained preparations, the choice of labeling antibody proved to be a limiting factor as we observed that sometimes, in tumor buds and poorly differentiated tumor areas, the tumor marker either lost its expression or showed a heterogeneous expression. This phenomenon has also been reported by other studies in the case of poorly differentiated tumors or tumors in advanced stages of evolution or that showed a molecular phenotype with high MSI [17, 18].

Therefore, it is necessary to test other antibodies that allow increasing the accuracy of tumor bud identification.

The use of IHC labeling also allowed us to experiment with automated identification of labeled features using dedicated image analysis modules designed for this study.

We initiated this endeavor because the literature has shown that the increasing implementation of digital pathology and artificial intelligence in CRC has generated a growing interest in automated assessment of TB, especially in the context of tumor heterogeneity and interobserver variability. There are studies that have explored the application of machine learning and deep learning algorithms to identify and quantify tumor buds on both H&E-stained and immunohistochemically labeled slides [19–21].

In the end, we can conclude that optimized IHC detection methods can provide suitable conditions for automated image analysis due to improved visualization of isolated tumor cells and clearer separation from surrounding stromal and inflammatory components, potentially facilitating the development of more reproducible and standardized digital TB assessment systems.

Conclusions

Our comparative study of tumor bud identification using two staining techniques demonstrated that, although conventional H&E assessment is considered the "gold standard" for TB identification according to current *ITBCC* recommendations, IHC labeling facilitated the visualization of isolated tumor buds and small tumor clusters, especially in difficult cases presenting stromal reactions or inflammatory infiltrates, and allowed the experimentation of successful automated tumor bud identification using dedicated image analysis programs on digitized histological slides.

Therefore, we would suggest that IHC labeling should be considered primarily as a detection tool, useful mainly in selected or equivocal cases, thus replacing routine H&E evaluation, but other antibodies should be tested to increase the accuracy of tumor bud identification.

Conflict of interests

The authors declare that they have no conflict of interests.

Institutional Review Board Statement

The study was conducted according with the Declaration of Helsinki and was approved by the Ethics Committee of the University of Medicine and Pharmacy of Craiova, Romania (Approval No. 177/14.09.2023).

References

[1] World Health Organization (WHO) Classification of Tumours Editorial Board. Digestive system tumours. 6th edition, vol. 1, WHO Classification of Tumours, International Agency for Research on Cancer (IARC) Press, Lyon, France, 2025. https://publications.iarc.who.int/662

[2] Zhang H, Simmer F, Lugli A, Nagtegaal ID. Tumor budding as a risk factor for lymph node metastasis and local recurrence in pT1 colorectal cancer: a systematic review and meta-analysis. Gastro Hep Adv, 2025, 4(9):100713. https://doi.org/10.1016/j.gastha.2025.100713 PMID: 40761702 PMCID: PMC12320163

[3] Viñal D, Rueda-Lara A, Martinez-Perez D, Zwisler P, Garcia-Leal A, Ruiz-Gutierrez I, Jiménez-Bou D, Peña-Lopez J, Alameda-Guijarro M, Martin-Montalvo G, Perez-Wert P, Martínez-Recio S, Palacios ME, Ghanem I, Custodio AB., Gutiérrez-Sainz L, Feliu J, Rodriguez Salas N. Prognostic value of tumor budding in patients with stage II and III colon cancer: a single-institution experience. J Clin Oncol, 2023, 41(4 Suppl):247. https://doi.org/10.1200/JCO.2023.41.4_suppl.247

[4] Ueno H, Ishiguro M, Nakatani E, Ishikawa T, Uetake H, Matsuda C, Nakamoto Y, Kotake M, Kurachi K, Egawa T, Yasumasa K, Murata K, Ikawa O, Shinji S, Murotani K, Matsui S, Teramukai S, Tomita N, Sugihara K; SACURA Study Group. Prospective multicenter study on the prognostic and predictive impact of tumor budding in stage II colon cancer: results from the SACURA trial. J Clin Oncol, 2019, 37(22):1886–1894. https://doi.org/10.1200/JCO.18.02059 PMID: 31180819 PMCID: PMC6675595

[5] Lugli A, Kirsch R, Ajioka Y, Bosman F, Cathomas G, Dawson H, El Zimaity H, Fléjou JF, Hansen TP, Hartmann A, Kakar S, Langner C, Nagtegaal I, Puppa G, Riddell R, Ristimäki A, Sheahan K, Smyrk T, Sugihara K, Terris B, Ueno H, Vieth M, Zlobec I, Quirke P. Recommendations for reporting tumor budding in colorectal cancer based on the International Tumor Budding Consensus Conference (ITBCC) 2016. Mod Pathol, 2017, 30(9):1299–1311. https://doi.org/10.1038/modpathol.2017.46 PMID: 28548122

[6] Zlobec I, Bächli M, Galuppini F, Berger MD, Dawson HE, Nagtegaal ID, Lugli A. Refining the ITBCC tumor budding scoring system with a "zero-budding" category in colorectal cancer. Virchows Arch, 2021, 479(6):1085–1090. https://doi.org/10.1007/s00428-021-03090-w PMID: 33843013 PMCID: PMC8724067

[7] Pihlmann Kristensen M, Korsgaard U, Timm S, Frøstrup Hansen T, Zlobec I, Kjær-Frifeldt S, Hager H. Immunohistochemical analysis of tumor budding in stage II colon cancer: exploring zero budding as a prognostic marker. Virchows Arch, 2024, 485(4):691–701. https://doi.org/10.1007/s00428-024-03860-2 PMID: 38977466 PMCID: PMC11522105

[8] Martinez-Ciarpaglini C, Fernandez-Sellers C, Tarazona N, Roselló S, Huerta M, Roda D, Mongort C, Ferrández A, Navarro S, Cervantes A. Improving tumour budding evaluation in colon cancer by extending the assessment area in colectomy specimens. Histopathology, 2019, 75(4):517–525. https://doi.org/10.1111/his.13900 PMID: 31081121

[9] Gwerder M, Demir CS, Williams HL, Lugli A, Martinez CG, Kowal J, Khan A, Kirchner P, Koessler T, Berger MD, Weigert M, Zlobec I. CDX2 expression dynamics in tumor clusters: a morpho-molecular biomarker in rectal cancer pretreatment biopsies revealed by sequential immunofluorescence. Sci Rep, 2026, 16(1):10129. https://doi.org/10.1038/s41598-026-40005-8 PMID: 41723209 PMCID: PMC13022250

[10] Yu J, Li S, Xu Z, Guo J, Li X, Wu Y, Zheng J, Sun X. CDX2 inhibits epithelial–mesenchymal transition in colorectal cancer by modulation of Snail expression and β-catenin stabilisation *via* transactivation of PTEN expression. Br J Cancer, 2021, 124(1):270–280. https://doi.org/10.1038/s41416-020-01148-1 PMID: 33239678 PMCID: PMC7782852

[11] Bodmer N, Uth K, Mehmeti R, Demir CS, Stroka D, Ghaffari-Tabrizi-Wizsy N, Lugli A, de Wever O, Zlobec I, Tschan MP.

CDX2 loss in colorectal cancer cells is associated with invasive properties and tumor budding. Sci Rep, 2025, 15(1):24113. https://doi.org/10.1038/s41598-025-07278-x PMID: 40619482 PMCID: PMC12230109

[12] College of American Pathologists (CAP). Cancer Protocol Templates. Protocols and Guidelines, Cancer Protocols, CAP, Northfield, IL, USA, 2026. https://www.cap.org/protocols-and-guidelines/cancer-protocols/current-cancer-protocols/

[13] Gologan D, Ştefan AE, Militaru M, Sanda AC, Arjan S, Muşat S, Leavitt MO, Stan R. Quality assurance and cost reduction in histopathology laboratories using tissue microarrays. Vet Sci, 2023, 10(4):280. https://doi.org/10.3390/vetsci10040280 PMID: 37104435 PMCID: PMC10147037

[14] Ştefan AE, Gologan D, Nitescu DAM, Muşat S, Stan R, Sanda CA, Arjan S, Militaru M. Pre-processed tissue microarray biomimetic material – applications and benefits. Rev Rom Med Vet, 33(1): 26–32. https://agmv.ro/wp-content/uploads/2023/03/26_32_Stefan_Alina.pdf

[15] Landau MA, Zhu B, Akwuole FN, Pai RK. Histopathological predictors of recurrence in stage III colon cancer: reappraisal of tumor deposits and tumor budding using AJCC8 criteria. Int J Surg Pathol, 2019, 27(2):147–158. https://doi.org/10.1177/1066896918787275 PMID: 29992847

[16] Werling RW, Yaziji H, Bacchi CE, Gown AM. CDX2, a highly sensitive and specific marker of adenocarcinomas of intestinal origin: an immunohistochemical survey of 476 primary and metastatic carcinomas. Am J Surg Pathol, 2003, 27(3):303–310. https://doi.org/10.1097/00000478-200303000-00003 PMID: 12604886

[17] Hinoi T, Tani M, Lucas PC, Caca K, Dunn RL, Macri E, Loda M, Appelman HD, Cho KR, Fearon ER. Loss of CDX2 expression and microsatellite instability are prominent features of large cell minimally differentiated carcinomas of the colon. Am J Pathol, 2001, 159(6):2239–2248. https://doi.org/10.1016/s0002-9440(10)63074-x PMID: 11733373 PMCID: PMC1850596

[18] Lugli A, Tzankov A, Zlobec I, Terracciano LM. Differential diagnostic and functional role of the multi-marker phenotype CDX2/CK20/CK7 in colorectal cancer stratified by mismatch repair status. Mod Pathol, 2008, 21(11):1403–1412. https://doi.org/10.1038/modpathol.2008.117 PMID: 18587323

[19] Bokhorst JM, Nagtegaal ID, Zlobec I, Dawson H, Sheahan K, Simmer F, Kirsch R, Vieth M, Lugli A, van der Laak J, Ciompi F. Semi-supervised learning to automate tumor bud detection in cytokeratin-stained whole-slide images of colorectal cancer. Cancers (Basel), 2023, 15(7):2079. https://doi.org/10.3390/cancers15072079 PMID: 37046742 PMCID: PMC10093661

[20] Sajjad U, Chen W, Rezapour M, Su Z, Tavolara T, Frankel WL, Gurcan MN, Niazi MKK. Enhancing colorectal cancer tumor bud detection using deep learning from routine H&E-stained slides. Proc SPIE Int Soc Opt Eng, 2024, 12933:129330T. https://doi.org/10.1117/12.3006796 PMID: 38752165 PMCID: PMC11095418

[21] Su Z, Chen W, Leigh PJ, Sajjad U, Niu S, Rezapour M, Frankel WL, Gurcan MN, Niazi MKK. Few-shot tumor bud segmentation using generative model in colorectal carcinoma. Proc SPIE Int Soc Opt Eng, 2024, 12933:129330A. https://doi.org/10.1117/12.3006418 PMID: 38756441 PMCID: PMC11098595

Corresponding authors

Gheorghe Gindrovel Dumitra, Associate Professor, MD, PhD, Department of Family Medicine, University of Medicine and Pharmacy of Craiova, 2 Petru Rareş Street, 200349 Craiova, Dolj County, Romania; Phone +40722–524 044, e-mail: gindrovel.dumitra@umfcv.ro

Iancu Emil Pleşea, Professor, MD, PhD, Departments of Pathology, Carol Davila University of Medicine and Pharmacy, and Bagdasar–Arseni Emergency Clinical Hospital, 12 Berceni Road, Sector 4, 041915 Bucharest, Romania; Phone +40722–992 511, e-mail: emil.plesea@umfcd.ro

Received: May 28, 2026

Accepted: July 30, 2026